CHINESE JOURNAL OF PHYSICS VOL. 24, NO. 1 SPRING 1986

Optical Properties of Hydrogenated Amorphous Silicon

Gwo-Jen Jan (詹國禎)
Department of Electrical Engineering, National Taiwan University, Taipei, Taiwan 10764
and
Ying-Sheng Huang (黃鶯聲)
Department of Electronics Engineering and Technology, National Taiwan Institute of Technology Taipei, Taiwan 10772

(Received 10 May 1935)

An on-line microcomputer based rotating light pipe reflectometer **(RLPR)** has been set up. Using this system we have investigated the optical properties of hydrogenated amorphous silicon semiconductor materials. The experimental results of reflectivity $R(\omega)$ has been analyzed by the Kramers-Kronig method. The complex dielectric function $\epsilon(\omega)$ and the effective number of electron per single Si-atom have been calculated. The results show that Boron-doped hydrogenated amorphous silicon and thermal annealing improved the crystallinity.

I. INTRODUCTION

The. amorphous silicon (a-Si) has been the subject of many investigations on disorder system over the past 15 years. The amorphous forms of this single elemental semiconductor is chosen because. of the throughly characterized and relatively well-understood crystalline properties. However, a-Si film generated made by sputtering (1) or electron beam techniques (2) contain a large density of states in the dangling bonds (1), and resulting large density of states in the energy gap makes it very difficult to move the Fermi level.

W. E. Spear and P. G. Le Combere (3) haved observed that glow discharged-produced a-Si possessed a relatively low density of gap states as compare to sputtered or evaporated film. It is now clear that these films are actually a amorphous silicon alloy and currently refered to as hydrogenated amorphous silicon (a-Si:H) films. The density of states in the energy gap of a-Si:H is relatively low, and thus the Fermi level can be moved with respect to the band edges by adding small quantities of certain dopants such as boron and phosphorous (4,5) as well as arsenic (7) have reported that the hydrogen evolution and annealing behavior is strongly modified if addtional structure defects are present due to boron doping.

The sharp features in the optical spectral of semiconductors are determined by long range order and hence are quite sensitive to disorder. The most of optical investigations have been confined to the region around the absorption edge (l-3 eV), (8,9). The di-

electric functions and optical parameters of elemental and III-V alloy semiconductors have been studied by Aspnes (10) et al. using the spectroscopic ellipsometer. The optical properties and damage analysis of GaAs single crystals partly amorphous by ion implementation were studied by the same technique (11). Unfortunely, spectroscopic ellipsometer can only provide the information of the optical properties in the energy range 1.0–6.0 eV. In constrast only a few results about the intensive studies on the gap states above the ultraviolet (UV) have been reported. Therefore, the reflectance spectroscopy over the wide energy range (0.8– 10 eV) will provide a considerable important tool to investigate thr properties of amorphous semiconductor.

Weiser et al. (12) have studies the reflectivity and the imaginary part of the dielectric function ϵ_2 over the photon energy range l-l 0 eV of glow-discharge silicon fabricated under different conditions. A broad bump, featureless in the imaginary part of the dielectric function ϵ_2 spectrum has been reported. The effects. of laser annealing on ion-damage silicon have been investigated by Aspnes (13). He found the energy features in ϵ_2 can be associated with crystalline silicon. Thus, the optical properties in UV region arise from the transitions between the band structure. These transition response is due to structure changes and/or randomly distributed impurities.

In order to study the boron doping and high temperature thermal annealing effect of a-Si:H samples, we have set up an automatic rotating light pipe reflectometer to measure the reflectivity spectral of the samples. The imaginary part of the dielectric function is calculated by the Kramers-Kronig analysis. The effective electron number per Si atom is also calculated from the dielectric function. In this paper the results of high temperature thermal annealed as well as unannealed a-Si:H(B) are reported. The detail structure in ϵ_2 of these samples will provide the information of the crystallinity improvement of silicon. For comparison we have also carried out the reflectance spectrum of the crystalline silicon.

II. THEORETICAL CONSIDERATION

The linear response of non-magnetic solid with isotropic or cubic symmetry to incident photon can be described in terms of two optical constants. These two optical constants (ϵ_1, ϵ_2) or (n, k) are related by the Kiamers-Kronig dispersion relations. It is more useful to express the dispersion relation between r, the magnitude of R, and the phase angle θ (w):

$$r(\omega) = R(\omega) \exp[i\theta(\omega)] \tag{1}$$

$$\theta(\omega) = \frac{\omega}{\pi} P \int_0^{\infty} \frac{[\ln R(\omega') - \ln R(\omega)]}{\omega^2 - \omega'^2} d\omega \tag{2}$$

where r is a complex reflection coefficient and $\theta(\omega)$ is the phase angle. The two optical constants n and k can be obtained fron R(w) and $\theta(\omega)$ by the following relations:

$$n(W) = \frac{1 - R}{1 + R - 2\sqrt{R}\cos\theta} \tag{3}$$

$$k(\omega) = \frac{2\sqrt{R}\sin\theta}{1 + R - 2\sqrt{R}\cos\theta} \tag{4}$$

If the reflectivity spectrum $R(\omega)$ is measured over the entire spectrum region, $\theta(\omega)$ can be calculated by the numerical computation for the spectrum region. Once the value of $\theta(\omega)$ is obtained, then two optical constants n, k can be calculated by eq. (3) and eq.(4). The real and imaginary part of the dielectric function are also calculated from the relations of the optical constants n, k as well as the absorption coefficient.

The numerical analysis of the Kramers-Kronig method is done by the integration of the eq. (2). The reflectivity $R(\omega)$ is measured only in a limited range of energies from 1.2 to 9.5 eV. In order to obtain the reflectivity $R(\omega)$ at lower energy (i.e. < 1.2 eV) and the higher energy (i.e. > 9.5 eV), the following extrapolation method is used in this numerical analysis. In the case of semiconductor, the reflectivity for photon energy E below the fundamental band gap Eg equal $(n-1)^2/(n+1)^2$. That means we chose $k \sim 0$ for $E < Eg$.

For the interpolation $R(\omega)$ at the higher energy region the following formula is used

$$R(\omega) \simeq R_u \left(\frac{\omega_u}{\omega}\right)^{\gamma} \tag{5}$$

where R_u is the reflectivity at the uper limit of the measurable photon energy $\hbar\omega_u$.

In our case, the measurable highest energy is about 9.5 eV, i.e., $\hbar\omega_u = 9.5$ eV. The pamameter is varried in order to obtain the values of n and k such that $k \approx 0$ for $\hbar\omega < Eg$. Above the energy $\hbar\omega_u$, the integration formula of the phase integral from $\hbar\omega_u$ to infinite is

$$\theta(\omega) = \frac{1}{2\pi}\ln\frac{R(\omega)}{R(\omega_u)}\ln\left|\frac{\omega_u + \omega}{\omega_u - \omega}\right| + \frac{\gamma}{m}\sum_{m=1}^{\infty}\frac{1}{(2m+1)^2}\left(\frac{\omega}{\omega_u}\right)^{2m+1} \tag{6}$$

where, m is the integer number.

This summation is performed to 50 terms in the program. The numerical calculation is carried out by the trapezoidal method. The value of γ is varried from 0 to 5. We chose the value of γ such that $k \approx 0$ (or $\epsilon_2 \approx 0$) for $E < Eg$.

III. EXPERIMENTAL APPARATUS AND SET UP

We have set up a microcomputer-based rotating light pipe reflectometer. The microcomputer system is used as a controller of rotating light pipe and monochromator. It is also used for real time data accqusition, manipulation and numerical analysis. We are carried the optical reflectance spectrum of unannealed and high temperature thermal annealed of a-Si:H alloys as well as c-Si sample over an energy range of 1.2 to 5.5 eV at near-normal incidence. The reflectivity spectrum of the samples within vaccum ultraviolet (VUV) photon energy region (5.5 – 9.5 eV) were measured at the Physics Department of the Brooklyn college.

The details about rotating light pipe reflectometer apparatus are found in the literature (15–16). The schematic functional block diagram of our system is shown in Fig. (1). The monochromator and predisperser used are Mc/Pherson GCA model 218 and model 608/218, respectively.

The different light sources are used in the whole spectral range of measurement. The

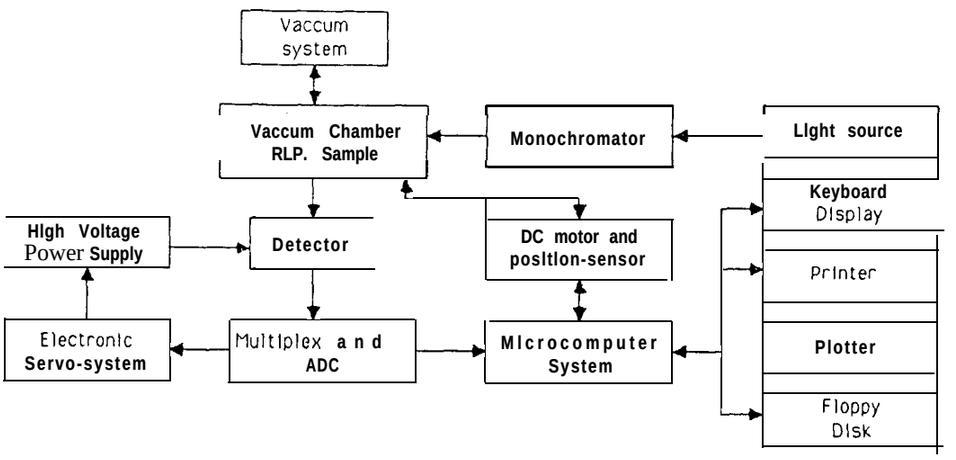

FIG. 1 Schematic functional block diagram of automatic RLPR System

hydrogen arc lamp is used in the VUV and UV region. A 150 watt Xenon arc lamp is used in the UV and visible light region. The Halogen Tungstan fused quartz lamp is used in the visible and near infra-red (IR) light range. The optical components and electro-optical devices used in our system is listed in table I.

TABLE I: E-O and Optical components related to measuring wavelenght

Wavelength (Å) / Components	5500 - 12000	2500 - 9000	1300 - 3500
LIght Source	TungstanQuartz Lamp	150 Watt Xe - Arc Lamp	1 K Watt Hydrogen Arc Lamp
Diffraction Grating Grove Density(G/mm)	600	1200	2400
Dirrraction Grating Blaze Wavelength	5000 Å	5000 Å	1500 Å
Pre-disperser (Prism)	GCA Model 608	GCA Model 608	No
Monochromator	GCA Model 218	GCA Model 218	GCA Model 218
Detectors (PMT)	S - 1	S - 20	S-20+phosphorous
Vaccum System	NO	No	$1 * 10^{-6}$ torr Yes

The photon detectors used in our measurement are Hamamatsu photomultiplier tube (PMT) S-l and S-20. The S-l PMT is used for the photon energy lower than 3.0 eV and S-20 PMT is used over the photon energy of 1.5 to 5.5 eV. The front surface of the rotating light pipe (fuse quartz of supersil no. 1) is coated with the phosphorus (using sodium salicylate phosphorus) and S-20 PMT is used over the photon energy of 3 eV to 9.5 eV. The chamber is mounted inside the vaccum working chamber. The chamber is pumped

down to 1 * 10" torr for VUV region. The schematical block diagram of rotating light pipe set up is shown in Fig. (2). The absolute accuracy of reflectivity R(w) in our measurement system is around 2% but the relative accuracy of R(w) value is around 0.3%.

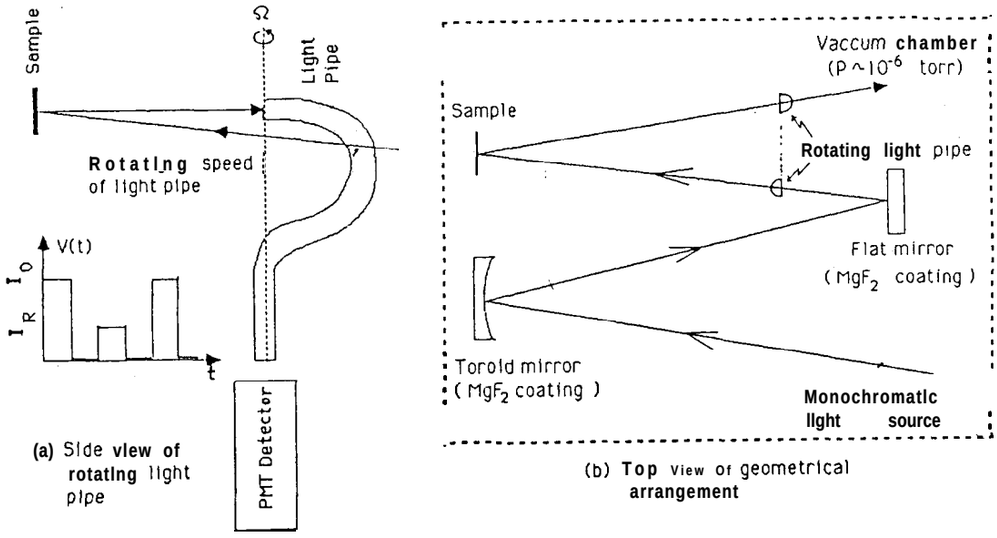

FIG. 2 The schematical block diagram of rotating light pipe set up

The samples used in this experiment were prepared by the glow-discharge technique. The characteristics and prepartion conditions are summarized and listed in table II. All samples are boron-doped a-Si:H alloy except c-Si. The doping concentration and annealing temperature are listed at the second and third column of table II. The samples have been annealed at temperature of ~ 1000" C for about 10 Min.

TABLE II. Summary of preparation condition for a-Si:H samples and experimental results

Sample	Doping		Annealing Temp. (°C)	Optical spectrum	EER Features
	Type	Concentration (ppm)			
#1	B	50	unannealed	Smooth bump	No
#2	B	50	1100	No structure for E_2	No
#3	B	500	900	Structure for E_2	Yes
#4	B		1000	Structure for E_2	Yes
c-Si	—	—	—	E_0', E_1, E_2, E_1'	Well-Resolved Structure

IV. EXPERIMENTAL RESULTS AND DATA ANALYSIS

We have measured the reflectivity of c-Si and a-Si:H(B) samples at room temperature carried out by our measurement system. The experimental results are shown in Fig. (3) and Fig. (4). The imaginary part of the dielectric function is calculated from the measured

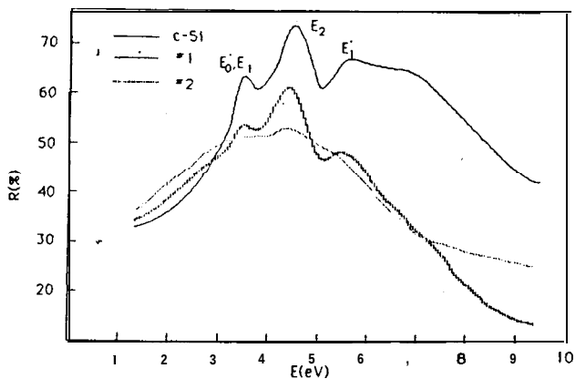

FIG. 3 The reflectance spectra for high temperature annealing a-Si:H(B), unannealed a-Si:(H) and c-Si.

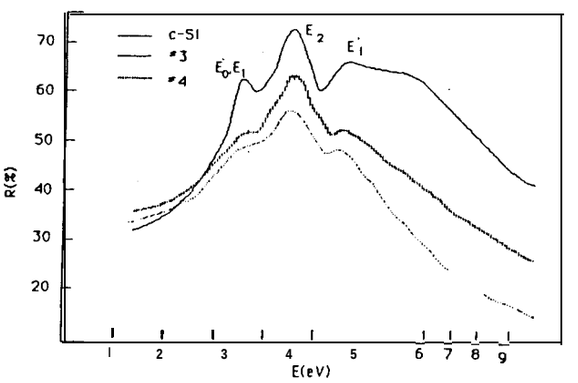

FIG. 4 The ' reflectance spectra for high temperature annealing a-Si:H(B), and c-Si.

reflectivity spectrum using Kramers-Kronig analysis and shown in Fig. (5) and Fig. (6). The effective electron number per single Si-atom is calculated from the imaginary part of the dielectric function ϵ_2 and shown in Fig. (7).

In Fig. (3) shows the reflectivity spectra of the unannealed and high temperature thermal annealed boron-doped with 50-PPM concentration as well as c-Si. The ϵ_2 spectral of those samples are shown in Fig. (5). The reflectivity and ϵ_2 spectra of the c-Si agree closely with Philip ' s results (1 5 – 17). The reflectance and the ϵ_2 spectra of the unannealed boron-doped a-Si:H sample shows a featureless broad bump spectra. This is similar to Weiser ' s result (12, 18). The samples of the high temperature thermal annealed a-Si:H(B) shows the little optical feature at E_0', E_1 and E_1' transition not well resolved feature at E_2 in

ϵ_2 spectrum.

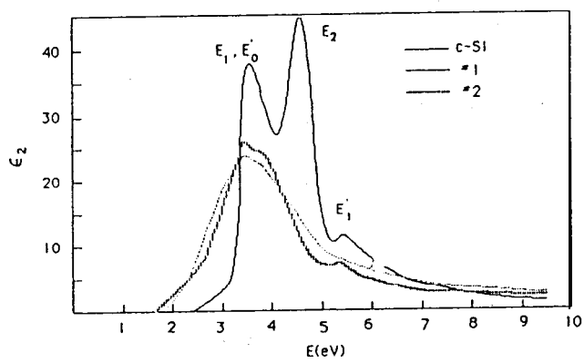

FIG. 5 The imaginary part ϵ_2 (E) of the dielectric function for high temperature annealing a-Si:H(B), unannealed a-Si:H(B) and c-Si.

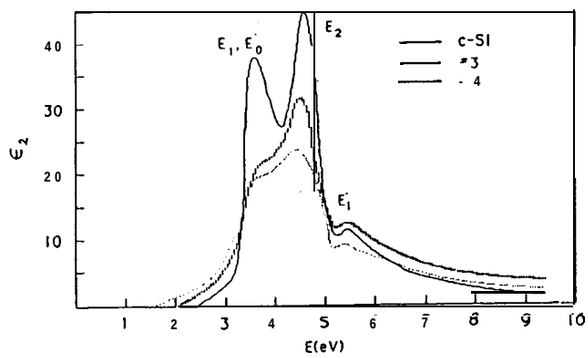

FIG. 6 The imaginary part ϵ_2 (E) of the dielectric function for high temperature annealing a-Si:H(B), and c-Si.

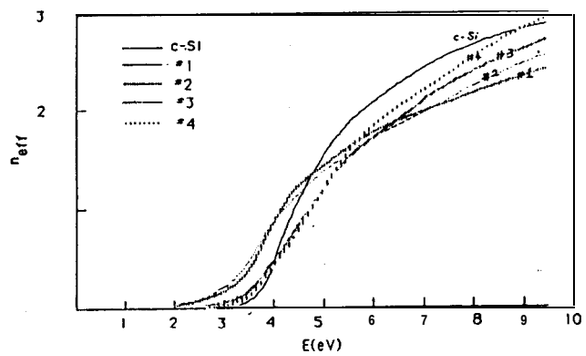

FIG. 7 The effective number of electron per atom contributing to optical absorption.

Figure (4) and Fig. (6) show the reflectance and ϵ_2 spectra of the high temperature thermal annealed a-Si:H with heavify boron-doped alloy. In Fig. (5) presents the little

optical features at E_0', E, transition resolved features at E_2 and E_1' energy position.

Figure (7) shows the effective electron number per single Si-atom calculated from the imaginary part of the dielectric function. The experimental results are summarized in table II.

V. DISCUSSIONS AND CONCLUSION

The most striking observation by comparing the optical spectra of a-Si and c-Si is the complete loss of fine structure in the disordered state. The fine structure is related to the singularities of the band structure and depends quite sensitive on the long range order in the material. These features are broaden rapidly with the loss of long range order (12). The featureless broad bump in ϵ_2 spectrum will present in amorphous state due to the short range order. The fine structure in reflectivity and ϵ_2 spectra show the more informations about the crystalline state. The imaginary part of the dielectric function provide the detailed information about the crystalline improvement of the a-Si:H alloy.

No fine structure in ϵ_2 spectrum is found in the sample #1. It indicates that the unannealed a-Si:H alloy with low concentration of boron-doped exhibits the amorphous state. The reflectivity and ϵ_2 spectra of the sample #2 show the fine structure at E_0', E_1 and E_1' transition but not well resolved fine structure at E_2 transition. It presents the short range order rather than the long range order. The crystallinity of a-Si:H(B) improved by the high temperature thermal annealing. This results have shown by the report of R. Tsu et al. using Raman characterization technique (19).

The reflectance and ϵ_2 spectra of samples #3 and #4 show the fine structure at critical points clearly. These optical features are from interband transition at the critical points. The annealing temperature of samples #3 and #4 are the same as sample #2 except the higher concentration of boron impurity. W. Beyer et al. (7) have shown the structure defecs can be modified by the thermal annealing and/or boron-doped. Electrolyte electroreflectance (EER) technique is a powerful tool to determine the optical transitions at critical point rapidly (20-2 1). When we check the EER spectrum of our measured samples, we found only sample #3 and #4 presented the EER energy features. But these features are not as fine and narrow as c-Si sample.' This evidences support that the high terpeiature thermal annealing and heavily boron-doped will improve the crystallinity of a-Si:H alloy. The major difference between samples #3 and #4 and c-Si is the E_1, E_0' features which are greatly depressed in the former materials. This effect may be related to the presence of a large number of free carriers. Aspnes (13) has also found that a depression of the 3.4 eV structure relative to E_2 in heavily-doped silicon. Our results indicate the high temperature thermal annealed and heavily boron-doped a-Si:H alloy is sufficient to obtain a high degree of structure order. This result is quite different compared with heavily n-doped hydrogenated ' and fluorinated amorphous silicon (a-Si:F:H) alloy which formed the microcrystalline structure (2 1).

Because of a shift of the joint density of the states the change of the short range order

should also alter the optical transition elements. These changes are repsonsible for the large variation of the height of the peak (7). Thus we calculated the effective number $n_{eff}(\omega)$ of electrons per single Si-atom excited at given photon energy $\hbar\omega$. For c-Si n_{eff} rises deeply above the direct energy band gap near 3 eV and saturated outside the range plotted here between 16 to 20 eV at a value of 4 corresponding to the 4 valence electron (20). The lower value of n_{eff} can be due to decreasing optical transition matrix element. The same observation has been reported by Bauer (23) for c-Si and amorphous germanium. He interpreted the lack of oscillator strength as an increasing localization of the deeper valence states in the disordered solid. The sample #1 exhibits the amorphous phase and has the lower value of the n_{eff} than samples #2, #3, #4. The n_{eff} value of the sample #2 is between that of samples #1 and #3. That means the crystallinity of the samples #3 and #4 is better than #1 and #2. The dopant of boron may play an important role in a-Si:H alloy as well as high temperature thermal annealing process.

ACKNOLEDGEMENT

We would like to thank professor Fred H. Pollak at the physics department of the Brooklyn college of the City university of New York to provide the samples and facilities of the VUV range measurement. We also like to acknowledge the National Science Council supported this research project under contract no. NSC-73-0204-M002-02 and NSC-74-0208-M1002-19.

REFERENCES

1. M. H. Brodsky and R. S. Tittle, Phys. Rev. Lett. 23, 581 (1969).
2. D. Beaglehole and M. Zavetova, J. NonCryst. Solids 4, 272 (1970).
3. W. E. Spear and P. G. Le Comber, Solid State Commun. 17, 1193 (1975).
4. W. E. Spear and P. G. Le Comber, J. Non-Cryst. Solids 8-10, 727 (1972).
5. D. E. Carlson, U. S. Patent No. 4,064 521 (1977).
6. J. C. Knights, J. M. Hayes, and J. C. Mikkelsen, Jr., Phys. Rev. Lett. 39, 712 (1977).
7. W. Beyer and H. Wagner, J. of Non-Cryst. 59-60, 161 (1963).
8. G. E. Jellison and F. A. Modine, Phys. Rev. (B) 27, 7466 (1983).
9. W. B. Jackson, D. K. bieglesen, R. J. Nemanich and J. C. Knights, Appl. Phys. Lett. 42, 105 (1983).
10. D. E. Aspnes and A. A. Atudna, Phys. Rev. (B) 27,985 (1983).
11. M. Erman, J. B. Theeten, P. Chambon, S. M. Kelso, and D. E. Aspnes, J. Appl. Phys. 56, 2664 (1984).
12. G. Weiser, D. Ewald, and M. Milleville, J. of Non-Cryst. Solids 35-36, 447 (1980); Phil. Mag. B40, 29 1 (1979).
13. D. E. Aspnes, Proc. and Symp. on Laser and Electron Beam Processing of Electronic

Materials, eds. C. L. Anderson, G. K. Cellar and G. A. Rozgonyi, (Electro-Chemical Society, Princeton, 1980) pp. 414.
14. See, for example, M. L. Theye in Optical Properties of Solids – New Developments, ed. by B. 0. Seraphin (North Holland, N. Y., 1976) pp. 335, and references therein.
15. H. R. Phillip and H. Ehrenerich, Phys. Rev. 129, 1550 (1963).
16. H. R. Phillip and H. A. Taft, Phys. Rev. 120, 37 (1960).
17. H. R. Phillip, J. Phys. Chem. Solid, 32, 1935 (1971).
18. D. T. Pierce and W. E. Spicer, Phys. Rev. B5, 3017 (1972).
19. R. Tsu, S. S. Chao, M. Izu, S. R. Ovshinsky, G. J. Jan and Fred H. Pollak, Proc. of the 9-th Intl. Conf. of Amorphous And Liquid Semicond., Grenohle, France (198 1).
20. F. H. Pollak, in Proc. of the Soc. of Photo-Optical Instrumentations Eng., Bellingham, Washington, 276, 142 (198 1).
21. M. Cardona, Modulation Spectroscopy, Academic Press, New York (1969).
22. G. J. Jan, F. H. Pollak and R. Tsu Solar Energy Materials, 8, 241 (1982).
23. R. S. Bauer, Proc. 5th Int. Conf. Amorphous and Liquid Semiconductors, Garmisch – Partenkirchen, pp. 595 (1973).